Towards Surface Analysis on Diabetic Feet Soles to Predict Ulcerations Using Photometric Stereo

Chanjuan Liu[a], Ferdi van der Heijden[a] and Jaap J. van Netten[b]

[a]Signals and Systems Group, Faculty Electrical Engineering, Mathematics and Computer Science, University of Twente, The Netherlands
[b]Department of Surgery, Hospital Group Twente, Almelo, The Netherlands

ABSTRACT

Diabetic foot ulceration is a major complication for patients with diabetes mellitus. Approximately 15% to 25% of patients with Type I and Type II diabetes eventually develop feet ulcers. If not adequately treated, these ulcers may lead to foot infection, and ultimately to total (or partial) lower extremity amputation, which means a great loss in health-related quality of life. The incidence of foot ulcers may be prevented by early identification and subsequent treatment of pre-signs of ulceration, such as callus formation, redness, fissures, and blisters. Therefore, frequent examination of the feet is necessary, preferably on a daily basis. However, self-examination is difficult or impossible due to consequences of the diabetes. Moreover, frequent examination by health care professionals is costly and not feasible. The objective of our project is to develop an intelligent telemedicine monitoring system that can be deployed at the patients' home environment for frequent examination of patients feet, to timely detect pre-signs of ulceration. The current paper reports the preliminary results of an implementation of a photometric stereo imaging system to detect 3D geometric abnormalities of the skin surfaces of foot soles. Using a flexible experimental setup, the system parameters such as number and positions of the illuminators have been selected so as to optimize the performance with respect to reconstructed surface. The system has been applied to a dummy foot sole. Finally, the curvature on the resulting 3D topography of the foot sole is implemented to show the feasibility of detecting the pre-signs of ulceration using photometric stereo imaging. The obtained results indicate clinical potential of this technology for detecting the pre-signs of ulceration on diabetic feet soles.

Keywords: Photometric stereo imaging (PSI), Surface Normal Reconstruction, Surface Albedo, Diabetic Foot Ulceration, Pre-Ulceration Detection, Telemedicine

1. INTRODUCTION

Diabetes Mellitus (DM) is one of the most common chronic diseases in nearly all countries, and continues to increase in numbers and significance. There were 194 million people suffering from DM worldwide in 2004,[1] and this number is expected to grow to 439 million by 2030.[2] Moreover, many patients with DM are affected by vascular and neurological complications in lower extremities. These conditions significantly increase the risk of developing foot ulcers. Approximately 15% to 25% of patients with DM eventually develop foot ulcers.[3] If not adequately treated, these ulcers may lead to foot infection, and ultimately to total (or partial) lower extremity amputation, which means a great loss in health-related quality of life.

It has been shown that >85% of all lower extremity amputations in patient with DM resulted from foot ulcerations.[4] The onset of diabetic foot ulcers may be prevented by early identification and subsequent treatment of pre-signs of ulceration, such as callus formation, redness, fissures, and blisters. This early identification depends on frequent risk assessment, preferably on a daily basis especially for high-risk patients.[5] Even though risk assessment of diabetic patients and monitoring of foot status are part of international guidelines on the management and prevention of the diabetic foot,[5] frequent assessment is not always possible. Self-examination is difficult or impossible due to the consequences of the diabetes, and frequent examination by health care professionals is costly and not feasible. Thus, any initiative that may overcome these limitations, contribute

Further author information: (Send correspondence to Chanjuan Liu)
Chanjuan Liu: E-mail: c.liu@ewi.utwente.nl

Advanced Biomedical and Clinical Diagnostic Systems X, edited by Tuan Vo-Dinh, Anita Mahadevan-Jansen, Warren S. Grundfest, Proc. of SPIE Vol. 8214, 82141D · © 2012 SPIE
CCC code: 1605-7422/12/$18 · doi: 10.1117/12.907245

to automated detection of the early warning signs, and be non-invasive, non-interactive and easy in use should be supported and implemented in diabetic feet care.[6] The ultimate objective of our project is to develop an intelligent telemedicine monitoring system that can be deployed at the patients' home environment for frequent examination of the patients' feet, to detect pre-signs of ulceration in a timely manner.

To this end, 3D surface reconstruction is essential in our desired telemedicine system, which can reveal the local 3D deformations of the skin surface, and then provide the information about the surface textures. These textures are either caused by geometrical variations of the surface (e.g. papillary lines, fissures, abundant callus) or by radiometrical variations (i.e. pigment variations). The assumption is that these textures can help to detect the (pre-signs of) ulceration in time to avoid the ulceration. Although there are already some laser foot scanners of the surface deformation in foot orthotics, such kind of scanners always require the subjects to stand on the scanners or press the feet against the scanners. The pressure on the foot skin surface can affect the skin local geometry. Thus, a 3D surface acquisition technique which can obtain the foot images without pressure on the skin is preferable for detecting the local 3D surface textures. Therefore, photometric stereo imaging is implemented in our project, which is a well established and affordable technique for 3D surface reconstruction. There are two typical tasks for reconstruction from photometric stereo imaging, which are:

- surface normal and albedo reconstruction from several images (usually three or more) obtained with different illumination sources under the same view point (camera);
- visible 3D surface reconstruction from the surface normal.

Using this imaging setup, one can get not only the local 3D deformations of the surface, but also the color property variations of the surface. Both modalities can help to achieve small local textures that can be used to detect and classify (pre-signs of) ulcerations.

In this study, we have built an experimental setup for photometric stereo imaging, with 12 illumination sources and one color CCD camera. Based on the acquired color images and the reconstruction results, the necessary number of illuminations was determined for further processing. From the selected images, surface normal and albedo reconstructions were performed and the surface depth map from the reconstructed surface normal was obtained. Finally, a surface analysis on the resulted 3D topography of the foot sole was implemented to investigate the feasibility to distinguish the small local differences for detecting pre-signs of ulceration using photometric stereo imaging. The obtained results indicate clinical potential of this technology for detecting the pre-signs of ulceration on diabetic feet soles.

The rest of this paper proceeds as follows: in the next section, studies on predicting diabetic feet ulcerations and an overview of photometric stereo technique will be discussed. The photometric stereo imaging experimental setup and the image acquisition done with it can be found in Section 3, while the reconstruction procedure and results will be presented in Section 4. In Section 5, the analysis of the reconstructed surface is then provided, followed by a discussion about the implications, potentials and limitations in Section 6.

2. RELATED WORK

In this section, the studies on diabetic feet ulceration predictions with different imaging techniques will be reviewed. An overview of photometric stereo imaging technique and the reconstruction methods, as well.

2.1 Imaging Techniques on Diabetic Foot Ulceration Prevention

Pre-signs of ulceration in diabetic foot include redness, increased local skin temperature,[6] thickening of the skin, fissures, blisters and abundant callus formation, all of which are physical features that enable a physician to diagnose the foot and to locate risk areas.[3,5,7] So far, there are three different imaging techniques that are used in predicting the diabetic foot ulceration, which are infrared imaging, photographic imaging, and hyperspectral imaging.

Infrared Imaging Studies show that there is a relationship between increased temperature and foot complications in diabetes. Increased temperature may be detected up to one week before a foot ulceration forms. Foot temperatures vary between patients and depend on ambient temperature and level of activity.[8] Therefore, a standardized reference is required for defining 'increased temperature'. The most common used criteria is as follows: if the temperature difference of the corresponding area of the right and left foot is more than 2.2°C, there is a high risk of infection or ulceration on the diabetic feet. Pilot studies that have been done on temperature measurement for diagnosis of foot problems fall in three categories: *a*) infrared (`IR`) thermometer (local measurement),[6,9] *b*) liquid crystal thermography (`LCT`),[10,11] and *c*) traditional `IR` camera systems.[12] The studies indicate that the incidence of the foot ulcerations could be reduced, whereby the lower amputations. However, the researchers also admit that a further interpretation of the results requires more time and health care resources.[6] Moreover, although in the recent decade, much research has been done in this area, there are still no guidelines for thermal assessment of the diabetic foot disorders. There is merely limited usage of the thermal technique for diabetic feet in a handful of countries.[8,13]

Photographic Imaging A photographic foot sole imager for home monitoring purposes was developed and evaluated. This device consisted of a digital RGB camera, an illuminator and a transmitter/receiver incorporated into a plastic housing. Photographic images of the feet soles were acquired with a reproducible and calibrated camera. Within the project, a series of 15 devices has been manufactured and tested. The evaluation results show that ulcerations can be diagnosed from photographs in a valid and reliable manner, but that the detection of pre-signs of ulcerations was more difficult.[14,15] Besides, the resolution of the images were just about the limit to resolve the individual papillary lines on the foot sole. As a result, image registration and alignment of two consecutive images was thereby not accurate enough.[16,17] This hinders automatic image analysis based on change detection. The conclusion can be driven that the photographic images do not carry sufficient information for reliable, automatic diagnosis of foot complications in diabetic patients. Thus, a more sophisticated scanning system of the foot is required.

Hyperspectral Imaging Changes in large vessels and microcirculation of the diabetic foot play an important role in the development of foot ulcerations and their subsequent failure to heal. Actually, 10 to 40% of diabetic patients are affected by peripheral vascular disease. Studies indicate that for a diabetic patient, *a*) the hyperaemic response of the foot skin to heating or minor trauma, *b*) the endothelia and vascular smooth function, and *c*) the nerve function, are impaired, especially for patients with diabetic neuropathy.[7] These vascular impairments may increase the risk of ulcerations and prohibit the healing response.

In recent years, medical hyperspectral imaging technique was developed as a novel noninvasive diagnostic tool to quantify the haemoglobin oxygenation,[18–20] to predict diabetic ulceration incidence[18] or healing.[19,20] These studies indicate that the oxygen saturation of haemoglobin is lower in the foot skin of diabetic patients than that of healthy people. In presence of diabetic neuropathy, such abnormality is accentuated. Thus, oxygen delivery to the tissues is reduced. The conclusion from the pilot research is that the hyperspectral imaging has the capability to identify microvascular abnormalities and tissue oxygenation in the diabetic foot, and thus to predict ulceration incidence.

The studies described above were limited to the analysis of the oxygenation changes in diabetic feet. Recently, a forward[21] and inverse[22] method extended the analysis on hyperspectral imaging results of diabetic feet to simultaneously determine *a*) the melanin concentration, *b*) the thickness of the epidermis, *c*) the volume of the fraction, *d*) the scattering coefficient of the feet sole skin, and *e*) the oxygen saturation of the blood in dermis. Their methods work well in predicting the ulcerations under abundant callus.[23,24]

Some experts in diabetes still doubt whether the microvascular impairment is responsible for the diabetic feet ulcerations,[7] although they admit that revascularization can help to cure the microvascular abnormalities in diabetic foot. Therefore, hyperspectral imaging can be a promising, noninvasive diagnosis tool for diabetic feet ulceration, but still it needs more research and resources to prove that.

2.2 Overview of Photometric Stereo Technique

Photometric stereo imaging was first introduced for Lambertian surfaces reconstruction in which two images were used to solve the reflectance function for recovering the surface gradients.[25] Over the past three decades,

extensive researches on more robust methods have been reported. For the reason that the simple Lambertian model oversimplifies the performance of the objects in the real world, the resulted surface reconstruction can be erroneous, especially when highlights or shadows exist in the acquired images. Most of these studies focused on solving this inherent difficulties of the traditional photometric stereo technique.

Photometric stereo technique with four light sources was proposed and extended.[26–28] This method overdetermines the local surface orientation and albedo (three degrees of freedom) and the residual of some least-squares solution can be used to determine whether problematic intensities exist or not. However, these methods fail when there are two or more shadows for one pixel in the recordings. Moreover, they are sensitive to noise caused by violations to the Lambertian model.

In a five-source photometric stereo imaging system,[29] the highest and lowest intensities for each pixel was simply discarded to avoid highlight and shadows. However, it can cause a significant loss of useful information.

Based on the four-source method,[28] a six-source photometric stereo method was proposed[12,30] to make sure there are at least three lights illuminating every location on a unit illumination sphere. Besides, there is a double-check for the shadowed pixels so that the second shadow will not be a big problem in the reconstruction. The six-source photometric stereo method worked well for some simple, convex objects. But the authors admitted that additional light sources would be necessary for more complex objects. In 2010, a reconstruction algorithm with an arbitrary number of illuminants was proposed.[31] This is the reconstruction method used in our study. Details about this implementation can be found in Section 4.

So far, the photometric stereo imaging and reconstruction technique has been used in many applications, for example, face and fingerprints reconstruction and recognition in biometrics,[32–34] cartridge cases surface reconstruction in forensics,[35] surface reconstruction of artist paintings[36] and melanin segmentation in dermatology,[37] etc. But as to the authors' knowledge, there has been no study on detecting pre-signs of ulceration on diabetic foot using photometric stereo technique . Our study will concentrate on the relevance and possibilities of this method for this specific purpose.

2.2.1 Reconstruction Principle

For a point P on a Lambertian surface, with surface normal $\mathbf{n}$ and albedo ρ, the brightness of the surface point under each illumination i ($i = 1 \cdots K$; K is the number of the illuminations) can be described by the Bi-direction Reflectance Function (`BRDF`), as follows:

$$B_i(P) = \frac{\rho(P)\mathbf{n}(P)\mathbf{s}_i(P)}{|\mathbf{r}(P)|^2} \tag{1}$$

where $\mathbf{r}$ is the distance vector and $\mathbf{s}_i(P) = \mu_i \mathbf{l}_i(P)$ is the illumination vector, pointing from the point P to the illumination source. Here $\mathbf{l}_i(P)$ represents the illumination direction and μ_i is a parameter proportional to the strength of the light.

In photometric stereo imaging, we usually assume that both the camera and the light sources are set at infinity from the object surface. The coordinate system is chosen such that the imaging plane coincides with the $xy-$plane and the $z-$axis coincides with the optical axis, as shown in Figure 1. Assuming that the intensity of the pixel is proportional to the brightness, we get

$$\begin{aligned} I_i(x,y) = kB_i(x,y) &= k\frac{\rho\mathbf{n}(x,y)\mathbf{s}_i(P)}{|\mathbf{r}(P)|^2} \\ &= \rho(x,y)\mathbf{n}(x,y)\cdot k\mathbf{s}_i \\ &= \rho(x,y)\mathbf{n}(x,y)\mathbf{v}_i \end{aligned} \tag{2}$$

where k is the ratio and $\mathbf{v}_i = k\mathbf{s}_i$.

If the photometric stereo imaging system contains K different illumination sources, then for each point on the surface, we have

$$\mathbf{I}(x,y) = \rho(x,y)\mathbf{n}(x,y)\mathbf{V} \tag{3}$$

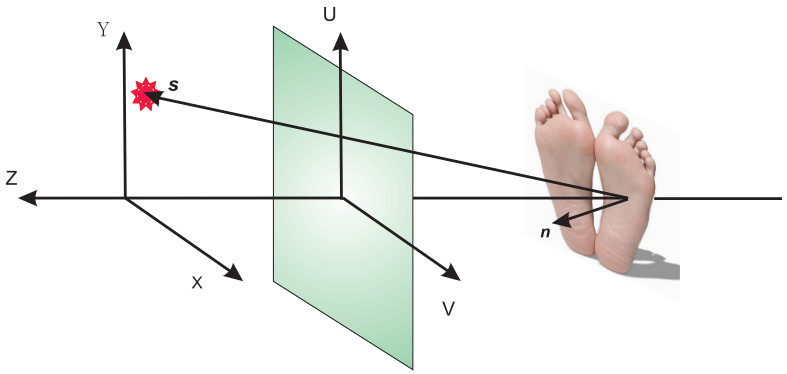

Figure 1. Model of the Scene Geometry

where $\mathbf{I}$ and $\mathbf{V}$ are the intensity matrix and the illumination matrix, respectively.

If the illumination vectors $\mathbf{s}_i$ do not lie in the same plane and $K = 3$, matrix $\mathbf{V}$ can be inverted, giving:

$$\mathbf{V}^{-1}\mathbf{I}(x, y) = \rho(x, y)\mathbf{n}(x, y) \tag{4}$$

Since $\mathbf{n}$ has unit length, one can estimate both the surface normal and albedo as follows:

$$\rho(x, y) = |\mathbf{V}^{-1}\mathbf{I}(x, y)| \tag{5}$$

$$\mathbf{n}(x, y) = \frac{1}{\rho}\mathbf{V}^{-1}\mathbf{I}(x, y) \tag{6}$$

If $K > 3$, the illumination matrix $\mathbf{V}$ is not square and cannot be inverted directly. The surface normal and albedo can be recovered following the least square estimation as:

$$\rho(x, y) = |(\mathbf{V}^T\mathbf{V})^{-1}\mathbf{V}^T\mathbf{I}(x, y)| \tag{7}$$

$$\mathbf{n}(x, y) = \frac{1}{\rho}(\mathbf{V}^T\mathbf{V})^{-1}\mathbf{V}^T\mathbf{I}(x, y) \tag{8}$$

We assumed that surface of the object can be described by a 2D height function $z = f(x, y)$. Let $g(x, y, z) = z - f(x, y) = 0$, then:

$$\nabla g(x, y, z) = -\frac{\partial f}{\partial x}\mathbf{i} - \frac{\partial f}{\partial y}\mathbf{j} + \mathbf{k} \tag{9}$$

For each point on the surface, we can define its gradient components as $p(x, y) = \frac{\partial f}{\partial x}$, $q(x, y) = \frac{\partial f}{\partial y}$, and the normal unit vector $\mathbf{n}(x, y)$ as:

$$\mathbf{n}(x, y) = \frac{(-p(x, y), -q(x, y), 1)}{\sqrt{p^2(x, y) + q^2(x, y) + 1}} \tag{10}$$

Then the surface heightmap can be evaluated as

$$f(u, v) = \int_0^u p\,\mathrm{d}x + \int_u^v p\,\mathrm{d}y \tag{11}$$

This heightmap provides us the reconstruction of the 3D surface.

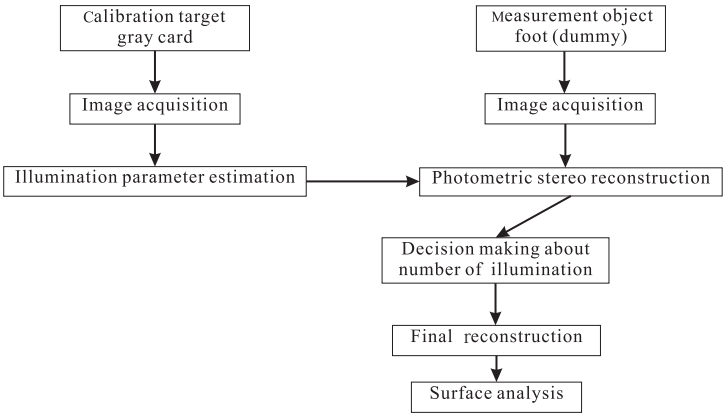

Figure 2. Flowchart of implementing photometric stereo imaging for detecting pre-ulceration signs on diabetic feet.

3. PHOTOMETRIC STEREO IMAGING SETUP

The objective of the experiments presented in this paper is to investigate whether the photometric stereo technique is capable of reconstructing the foot skin surface accurately. Using the reconstruction results, surface analysis can be done to determine whether it is sufficient for detecting local features on the feet surface and whether it has potential for observing the pre-signs of ulceration. To conduct the experiment, we employed a foot dummy as our measurement object. The basic steps of this study are given in Figure 2 and each steps will be discussed in the following sections.

The experimental setup was built as shown in Figure 3, using one 1600×1200 pixel CCD multi-spectral camera*, 12 illumination sources and a foot dummy as an object. A wide angle $f1.4/23mm$ lens is mounted in the camera so that the 1600×1200 image covers an area of $320mm \times 240mm$. The 12 power LED light sources are mounted on a circle and the tilt angles of the light sources are equally spaced around the circle. The diameter of the illumination circle is about $580mm$. In order to keep the slant angle of the illumination source in the interval of $30° \sim 45°$, the distance between the illumination plate and the foot dummy was set to be $400mm$. In that case the slant angle of all the illuminants are the same as $\approx 35°$. The measurement object, foot dummy, was built by shaping a mould around the foot of a living female volunteer with liquid latex. This substance has sufficiently low viscosity to model the fine surface relief. After the mould dried, it is filled with with white plaster. Finally, the surface of the dried plaster was painted with skin color. So the foot dummy is sufficient as a static measurement object for our experiment. During the image acquisition, the foot dummy is illuminated by one of the light sources each time and observed by the fixed camera.

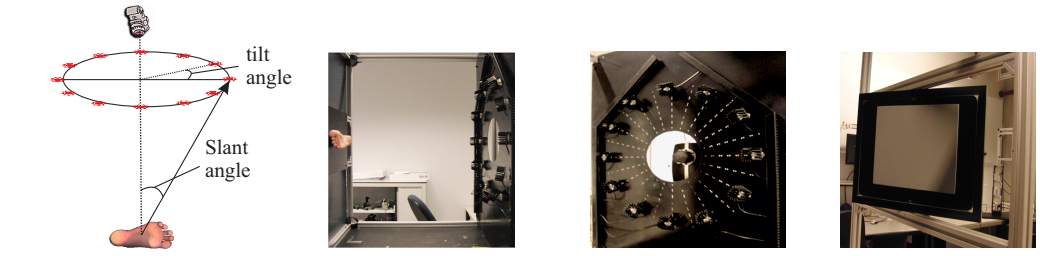

(a) Schematic of experimental setup with 12 illuminations

(b) Experimental setup for photometric stereo imaging

(c) Illumination plate and aperture for camera

(d) Example of tilting the gray card

Figure 3. Photometric imaging setup with 12 illuminants. The experiments were carried out in a dark room, so there is no influence from the ambient light.

For our experimental setup, the distance between the illumination plate and the object is not long enough to make sure the light is uniformly distributed on the target surface. Thus, a Kodak® R-27 18% gray card was

*Art Innovation ARTIST Multi-spectral camera, DEMCON Advanced Products BV, Oldenzaal, The Netherlands, www.art-innovation.nl

used to calibrate the light directions and brightness distribution on the surface before actual measurements took place. For a gray card, the surface normal and the albedo are already known. From Eq. 3, the illumination matrix $\mathbf{V}$ can be easily derived for each pixel on the gray card. During the calibration, the gray card was tilted to four different angels as, for example, shown in Figure 3-(d), having 30° to the vertical and/or horizontal plane. For every tilt angle, one image of the gray card would be taken under each illumination source.

4. SURFACE RECONSTRUCTION

We implemented the reconstruction algorithm proposed by Argyriou et al.[31] to obtain the reconstructed surface albedo and the 3D surface of the foot dummy with the images from our photometric stereo imaging setup introduced in Section 3.

The photometric stereo technique with an arbitrary number, K, illuminants was developed based on the 4-source photometric stereo method.[28] The assumptions are: for acquired gray-level images *a*) there is no ambient light present during the image acquisition, which is true for our case. *b*) There is only one highlight in all the K obtained pixel intensities from K different illuminants, and there can be more than one shadows present in the K pixel values. The flowchart of the algorithm can be found in Figure 4. For color photometric stereo reconstruction, the steps in the flow chart are repeated for each color channel. Theoretically, the three calculated values for a given surface normal should be the same. However, in practice there is usually some slight variation as there is always some noise in the acquired images.[37] To reduce the errors, the mean of the three calculated surface normal values is used as the reconstruction results. And then, the composite albedos can be recalculated using Eq.8 for each color channel.

As shown, there is an error check step for determining whether the K obtained intensities tuple for each pixel is problematic or not. The principle of this error check is that we have an over-determined system of equations. This offers the possibility of checking whether the residuals are not too large. This principle is implemented as follows: the vectors of the orthogonal basis of the illuminations space are stacked row-wise to form a $(K-3)\times K$ matrix, $\mathbf{A}$.

If we consider the K-tuple of the intensities which contains some errors $\mathbf{E}$:

$$\tilde{\mathbf{I}} = \mathbf{I} + \mathbf{E} = \mathbf{V}\rho\mathbf{n} + \mathbf{E} \tag{12}$$

And if we project the intensity matrix $\tilde{\mathbf{I}}$ to on this orthogonal subspace $\mathbf{A}$, we will have:

$$\mathbf{A}\tilde{\mathbf{I}} = \mathbf{AV}\rho\mathbf{n} + \mathbf{AE} \tag{13}$$

with $\mathbf{AV} = \mathbf{0}$, the projection of the intensity matrix actually is left with the projection of the errors $\mathbf{P} = \mathbf{AE}$.

According to the flow chart, a predefined threshold value in the check function is required to determine whether tuple of a pixel contains defected pixel intensities (shadowed or highlighted) or not. According to Argyriou et al.,[31] the threshold may need to be defined using set of training data. Barsky and Petrou stated in their four-source PSI that the threshold should be $T_V \approx 0.02 \sim 0.04$.[28] Thus, we chose $T_V = 0.03$ for our study here.

It is difficult to decide how many illumination sources are needed because we do not have ground truth for the measurement object. If the acquisition time is too long, the patient will move its foot during the image acquisition. This will cause motion artifacts between the images. And such artifacts are difficult to restore. Thus, we need to make the duration of the data acquisition as short as possible by means of reducing the number of illumination sources, while the reconstruction result is still sufficiently accurate. In this study, the number of illumination sources is determined using the reconstruction obtained with 12 illuminants as ground truth. Then the illumination sources were reduced to check the root mean square errors regarding to the 'ground truth'. The comparison results of the reconstruction with different combinations of the illumination source with different number of illuminants are shown in Figure 5, according to which the number of illumination was decided to be eight. The reconstruction was done with the chosen 8 illuminants and the corresponding images. The results are shown in Figure 6.

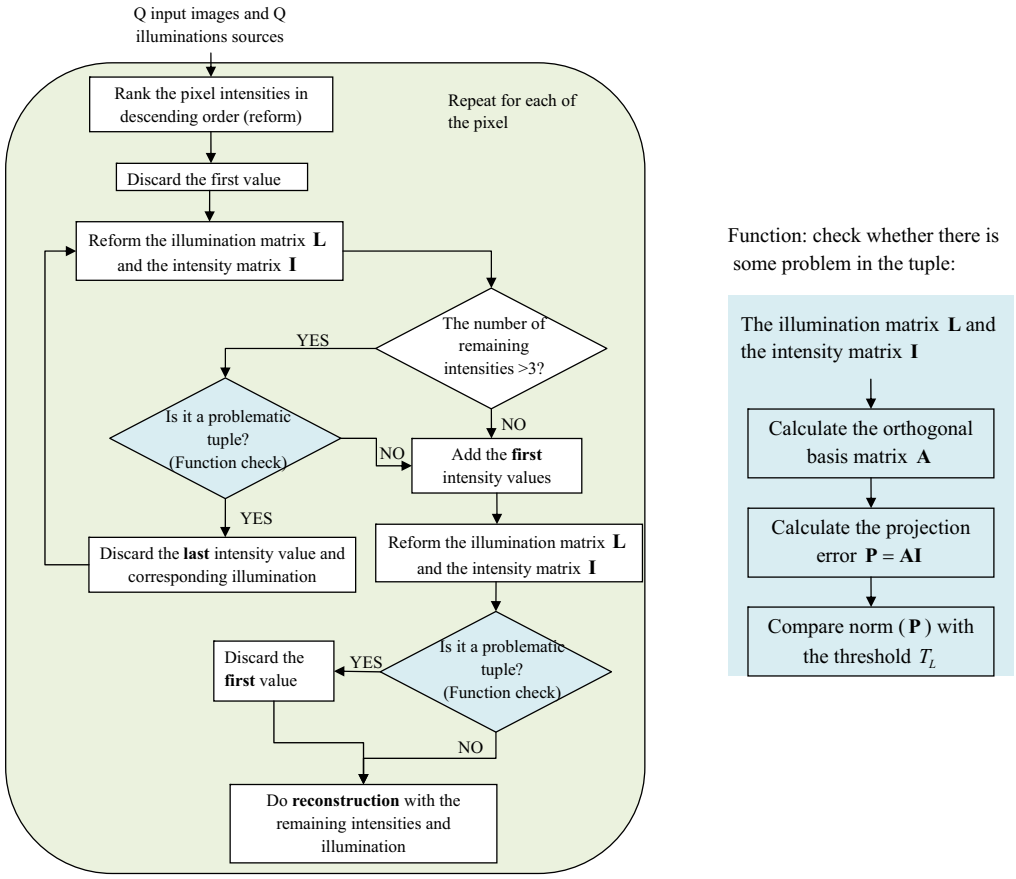

Figure 4. The flowchart of the photometric stereo reconstruction with arbitrary illuminants.

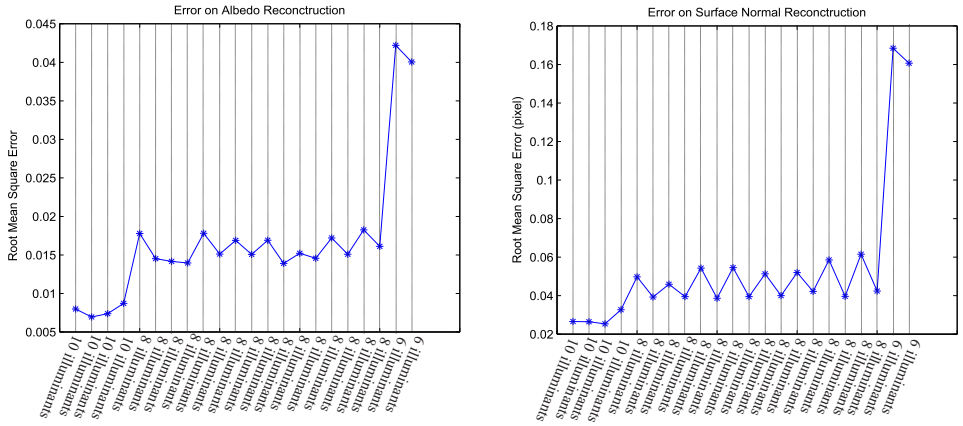

Figure 5. Root mean square errors for reconstructed albedos and surface normals with different combinations of different number of illuminants. The combinations of the illumination were chosen to make sure the illuminants symmetric. As shown, the errors for surface normal and albedo reconstructions with 10 illuminants are the least. For 8 illuminants, the errors increase by about 0.005 for albedo reconstruction and 0.01 pixel for normal reconstruction. But the errors for reconstruction with 6 illuminants increase dramatically (0.025 for albedo reconstruction and 0.12 pixel for normal reconstruction). To make a trade-off between the accuracy and the number of the illuminants, the fourth combination of 8 illuminants was chosen to do our reconstruction. In the near future the final setup will contain 8 symmetric illuminants on a circle.

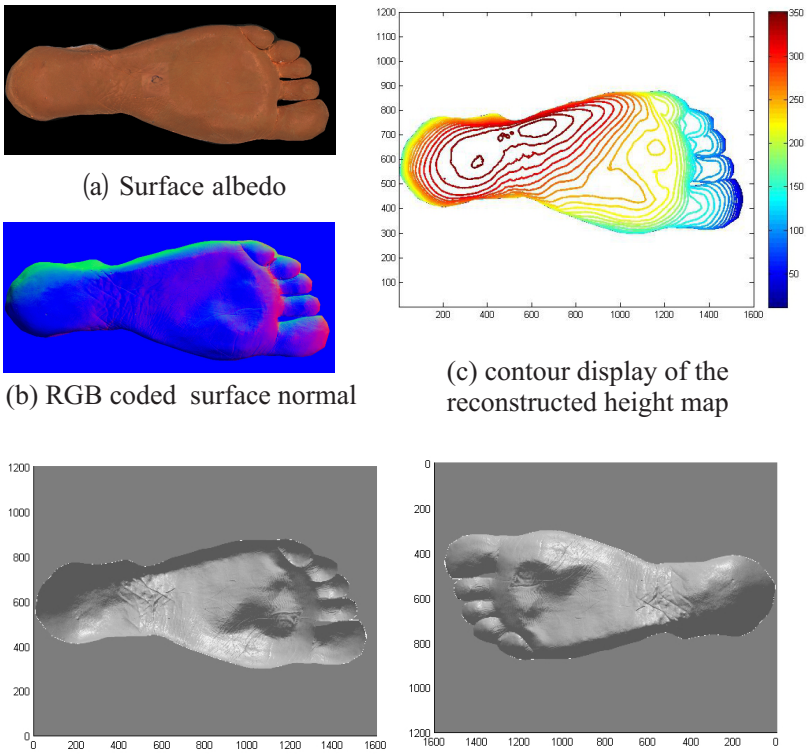

Figure 6. Reconstruction results. From the reconstructed albedo we can clearly see the color difference on the whole feet surface. Besides in the reconstructed 3D surface, the papillary lines can be observed as well as some small dimples on the surface of the foot dummy.

5. SURFACE ANALYSIS

The reconstructed 3D surface is rich in local structural features. Thus, the surface curvature maps, which uniquely characterize the local shape of a surface, are used as 3D representations. The surface curvature properties have been widely used to represent and recognize various surfaces. Properties such as mean and Gaussian curvatures are also used to classify points on a surface to different classes.[38,39]

For a surface patch represented by $X(u, v) = (u, v, f(u, v))$, Gaussian curvature (K) and mean curvature (H) are calculated as follows:

$$K(X) = \frac{f_{uu}f_{vv} - f_{uv}^2}{1 + f_u^2 + f_v^2} \quad and \quad H(X) = \frac{(1 + f_u^2)f_{vv} + (1 + f_v^2)f_{uu} - 2f_u f_v f_{uv}}{(1 + f_u^2 + f_v^2)^{3/2}} \tag{14}$$

where, f_u , f_v and f_{uu},f_{vv}, f_{uv} are first and second order partial derivatives of f(u, v). Once the values of K and H are found at every point on the 3D surface, the principal curvatures k_1 and k_2 can be determined as:

$$k_1, k_2 = H \pm \sqrt{H^2 - K} \tag{15}$$

In practice, these principal curvature values are computed at every pixel by fitting a Gaussian surface over a local neighborhood and then estimating the first and second derivatives of the surface. The window size of calculating the curvature need to be carefully chosen. When the size is too small, the curvature estimation will be sensitive to noise, while the size is too large, it can smooth the image and we will lose details on the surface. Empirically, the size of the window for our experiments was set as 7×7.

To represent the curvature of every point on the 3D surface of the foot sole by a scalar value, we utilized the curvedness (C) introduced in.[38] The positive value C is a measure of how sharply or gently curved a point is. It is defined in terms of principal curvatures k_1 and k_2 , as:

$$C = \sqrt{(k_1^2 + k_2^2)/2} \tag{16}$$

Thus a scalar value of curvature is obtained for every point on the 3D reconstructed surface and this can be stored in a 2D matrix and can be shown as an image, as Figure 7. From this, we can clearly see papillary lines and some holes (white spots on the foot sole) on the curvature of the foot sole which can be used as the feature for classification and feature matching in the future experiments with real patients' feet images.

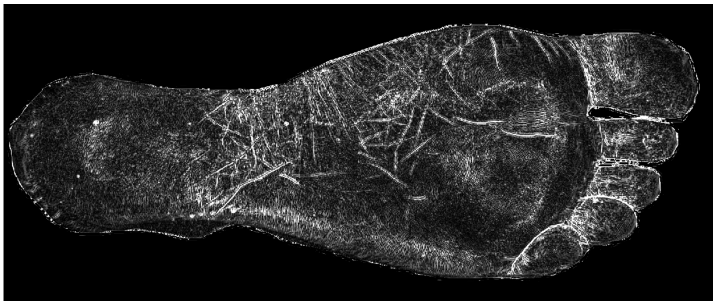

Figure 7. The surface Curvature obtained from the 3D surface reconstruction

6. DISCUSSION AND FUTURE WORK

In this paper, a brief introduction of our project was given first. Then, a review on the imaging techniques applied on predicting diabetic foot ulceration followed. To build an intelligent telemedicine system to detect the per-signs of ulceration automatically, a 3D surface acquisition technique is desirable. Such technique can reveal the local surface textures and then help to predict the diabetic foot ulceration. To this end, photometric stereo imaging is implemented in our project.

In this study, we have built an experimental setup to investigate the feasibility of applying photometric stereo imaging to reconstruct the 3D surface of feet by using a foot dummy as an object. So far, the surface reconstruction of the foot dummy (Figure 6) and the surface curvature analysis done on the reconstruction (Figure 7) are promising for detecting the local surface features. In Figures 6 and 7, the papillary lines and dimples on the surface of the foot dummy can be obviously observed. Thus, we can conclude that the 3D surface obtained from the photometric stereo imaging setup built in our lab is capable of capturing the surface textures using the reconstructed 3D surface.

In the near future, the photometric stereo imaging setup will be applied on real human feet to investigate the feasibility of this technique for lively foot images acquisition and reconstruction. In the meantime, the experimental setup will be further improved to make it more compact by reducing the number of illuminants, while the reconstruction results are still sufficient to detect the local surface textures. Finally, an experimental setup of photometric stereo imaging will be developed for clinical practice.

ACKNOWLEDGMENTS

This project is granted by public funding from ZonMw, the Netherlands Organisation for Health Research and Development. We appreciate the generous help from DEMCON Advanced Mechatronics BV (Oldenzaal, The Netherlands), especially Dr. Marvin E. Klein, for providing the camera and foot dummy, and suggestions during the experimental setup building.

REFERENCES

[1] Wild, S., Roglic, G., Green, A., Sicree, R., and King, H., "Global prevalence of diabetes: Estimates for the year 2000 and projections for 2030," *Diabetes Care* **27**, 1047–1053 (2004).

[2] Shaw, J. E., Sicree, R. A., and Zimmet, P. Z., "Global estimates of the prevalence of diabetes for 2010 and 2030," *Diabetes Research and Clinical Practice* **87**, 4–14 (2010).

[3] Singh, N., Amstrong, D. G., and Lipsky, B. A., "Preventing foot ulcers in patients with diabetes," *The Journal of the American Medical Association* **293**, 217–228 (2005).

[4] Boulton, A. J. M., "The diabetic foot: grand overview, epidermology and pathogenesis," *Diabetes/Metabolism Research and Reviews* **24**, S3–S6 (2008).

[5] Apelqvist, J., Bakker, K., van Houtum, W., and Schaper, N. C., "Practical guidelines on the management and prevention of the diabetic foot," *Diabetes/Metabolism Research and Reviews* **24**, S181–S187 (2008).

[6] Lavery, L. A., Higgins, K. R., Lanctot, D. R., Constantinides, G. P., Zamorano, R. G., Athanasiou, K. A., Armstrong, D. G., and Agrawal, C. M., "Preventing diabetic foot ulcer recurrence in high-risk patients: use of temperature monitoring as a self-assessment tool," *Diabetes Care* **30**, 14–20 (2007).

[7] Korzon-Burakowska, A. and Edmonds, M., "Role of the microcirculation in diabetic foot ulceration," *International Journal of Lower Extremity Wounds* **5**, 144–148 (2006).

[8] Roback, K., "An overview of temperature monitoring devices for early detection of diabetic foot disorders," *Expert Reviews of Medical Devices* **7**, 711–718 (2010).

[9] Lavery, L. A., Higgins, K. R., Lanctot, D. R., Constantinides, G. P., Zamorano, R. G., Armstrong, D. G., Athanasiou, K. A., and Agrawal, C. M., "Home monitoring of foot skin temperatures to prevent ulceration," *Diabetes Care* **27**, 2642–2647 (2004).

[10] Roback, K., Johansson, M., and Starkhammar, A., "Feasibility of a thermographic method for early detection of foot disorders in diabetes," *Diabetes Technology & Therapeutics* **11**, 663–337 (2009).

[11] Frykberg, R. G., Tallis, A., and Tierney, E., "Diabetic foot self examination with the tempstat™ as an integral component of a comprehensive prevention program," *The Journal of Diabetic Foot Complications* **1**, 13–18 (2009).

[12] Sun, P., Lin, H., Jao, S. H. E., Ku, Y. C., Chan, R. C., and Cheng, C. K., "Relationship of skin temperature to sympathetic dysfunction in diabetic at-risk feet," *Diabetes Research and Clinical Practice* **73**, 41–46 (2006).

[13] Bharara, M., Cobb, J. E., and Claremont, D. J., "Thermography and thermometry in the assessment of diabetic neuropathic foot: A case for furthering the role of thermal techniques," *International Journal of Lower Extremity Wounds* **5**, 250–260 (2006).

[14] Hazenberg, C. E., van Baal, J. G., Manning, E., Bril, A., and Bus, S. A., "The validity and reliability of diagnosing foot ulcers and pre-ulcerative lesions in diabetes using advanced digital photography," *Diabetes Technology & Therapeutics* **12**, 1011–7 (2010).

[15] Hazenberg, C. E., Bus, S. A., Kottink, A. I., Bouwmans, C. A., Schöbach-Spraul, A. M., and van Baal, S. G., "Telemedical home-monitoring of diabetic foot disease using photographic foot imaging - a feasibility study," *Journal of Telemedicine and Telecare* **24** (2011).

[16] Klein, A., *Alignment of Diabetic Feet*, Master's thesis, University of Twente; Signals and Systems Group, Enschede (2006). M.Sc. Report SAS2606.

[17] Klein, A., van der Heijden, F., and Slump, C. H., "Alignment of diabetic feet images," in [*Proceedings of SPS-DARTS 2007, the third annual IEEE Benelux/DSP Valley Signal Processing Symposium*], IEEE Benelux/DSP (2007).

[18] Greenman, R. L., Panasyuk, S., Wang, X., Lyons, T. E., Dinh, T., Longoria, L., Giurini, J. M., Freeman, J., Khaodhiar, L., and Veves, A., "Early changes in the skin microcirculation and muscle metabolism of the diabetic foot," *The Lancet* **366**, 1711–1717 (2005).

[19] Khaodhiar, L., Dinh, T., Schomacker, K. T., Panasyuk, S. V., Freeman, J. E., Lew, R., Vo, T., Panasyuk, A. A., Lima, C., Giurini, J. M., Lyons, T. E., and Veves, A., "The use of medical hyperspectral technology to evaluate microcirculatory changes in diabetic foot ulcers and to predict clinical outcomes," *Diabetes Care* **30**, 903–910 (2007).

[20] Nouvong, A., Hoogwerf, B., Mohler, E., Davis, B., Tajaddini, A., and Medenilla, E., "Evaluation of diabetic foot ulcer healing with hyperspectral imaging of oxyhemoglobin and deoxyhemoglobin," *Diabetes Care* **32**, 2056–2061 (2009).

[21] Yudovsky, D. and Pilon, L., "Simple and accurate expressions for diffuse reflectance of semi-infinite and two-layer absorbing and scattering media," *Applied Optics* **48**, 6670–6683 (2009).

[22] Yudovsky, D. and Pilon, L., "Rapid and accurate estimation of blood saturation, melanin content, and epidermis thickness from spectral diffuse reflectance," *Applied Optics* **49**, 1707–1719 (2010).

[23] Yudovsky, D., Nouvong, A., Schomacker, K., and Pilon, L., "Monitoring temporal development and healing of diabetic foot ulceration using hyperspectral imaging," *Journal of Biophotonics* **4**, 565–576 (2011).

[24] Yudovsky, D., Nouvong, A., Schomacker, K., and Pilon, L., "Assessing diabetic foot ulcer development risk with hyperspectral tissue oximetry," *Journal of Biomedical optics* **16**, (026009) 1–8 (2011).

[25] Woodham, R. J., "Photometric method for determing surface orientation from multiple images," *Optical Engineering* **19**, 139–144 (1980).

[26] Coleman, J. E. N. and Jain, R., "Obtaining 3-dimensional shape of textured and specular surfaces using four-source photometry," *Computer Graphics and Image Processing* **18**, 309–328 (1982).

[27] Solomon, F. and lkeuchi, K., "Extracting the shape and roughness of specular lobe objects using for light photometric stereo," *IEEE Transactions on Pattern Analysis and Machine Intelligence* **18**, 449 – 454 (1996).

[28] Barsky, S. and Petrou, M., "The 4-source photometric stereo technique for three-dimensional surfaces in the presence of highlights and shadows," *IEEE Transactions on Pattern Analysis and Machine Intelligence* **25**, 1239–1252 (2003).

[29] Rushmeier, H., Taubin, G., and Guéziec, A., "Applying shape from lighting variation to bump map capture," in [*Eighth Eurographics Rendering Workshop*], 53–44 (1997).

[30] Sun, J., Smith, M., Smith, L., Midha, S., and Bamber, J., "Object surface recovery using a multi-light photometric stereo technique for non-lambertian surfaces subject to shadows and specularities," *Image and Vision Computing* **25**, 1050–1057 (2007).

[31] Argyriou, V., Petrou, M., and Barsky, S., "Photometric stereo with an arbitrary number of illuminants," *Computer Vision and Image Understanding* **114**, 887–900 (2010).

[32] McGunnigle, G. and Chantler, M. J., "Recovery of fingerprints using photometric stereo," in [*In Proceedings of the Irish Machine Vision and Image Processing Conference (IMVIP'01)*], 192–199 (2001).

[33] Woodman, R., *A Photometric Stereo Approach to Face Recognition*, Master's thesis, University of the West of England (2007).

[34] Temizkan, E. and Bilge, H. S., "Shape index based 3d face recognition using photometric stereo," in [*2011 IEEE 19th Conference on Signal Processing and Communications Applications (SIU)*], 454–457 (April 2011).

[35] Sakarya, U., Leloğlu, U. M., and Tunali, E., "Three-dimensional surface reconstruction for cartridge cases using photometric stereo," *Forensic Science International Journal* **175**, 209–217 (2008).

[36] Hasegawa, T., Tsmura, N., Nakaguchi, T., and Iino, K., "Photometric approach to surface reconstruction of artist paintings," *Journal of Electric Imaging* **20**, (013006) 1–11 (2011).

[37] Sun, J., Smith, M., Smith, L., Coutts, L., Dabis, R., Harland, C., and Bamber, J., "Reflectance of human skin using colour photometric stereo - with particular application to pigmented lesion analysis," *Skin Research and Technology* **14**, 173–179 (2008).

[38] Woodham, R. J., "Gradient and curvature from the photometric-stereo method, including local confidence estimation," *Journal of optical society of America* **A 11**, 3050–3068 (1994).

[39] Zhang, D., Kanhangad, V., Luo, N., and Kumar, A., "Robust palmprint verification using 2d and 3d features," *Pattern Recognition* **43**, 358–368 (2010).